



# Effects of welding parameters on microstructure and mechanical properties of underwater wet friction taper plug welded pipeline steel

Junzhen Xiong<sup>1</sup> · Xinqi Yang<sup>1</sup> · Wei Lin<sup>1</sup> · Kaixuan Liu<sup>1</sup>

Received: 5 August 2017 / Accepted: 26 August 2018 / Published online: 7 September 2018  
© International Institute of Welding 2018

## Abstract

Microstructure and mechanical properties of underwater wet friction taper plug-welded API X52 pipeline steel with 6500–7500-rpm rotational speed at 30–45-kN axial force have been investigated, and the defect-free friction taper plug-welded joints were obtained. It was found that the microstructure in welded joint was remarkably inhomogeneous and very different from the X52 base metal. The weld region could be divided into forged zone (FZ), final frictional plane (FFP), shear deformation zone (SDZ), bonding zone (BZ), and heat-affected zone (HAZ). The HAZ has the coarsest grain and mainly consists of martensite and bainite, and the FZ and SDZ are mainly characterized by a mixture of martensite, bainite, and various shapes of ferrites. The BZ is represented by the banding pattern of fine equi-axed grain ferrites because of local decarbonization around frictional interface in wet welding condition. The axial force has a greater impact on microstructure of welded joint as compared with rotational speed. The hardness profiles measured on cross section of welded joints are severely non-uniform, ranging from 200 to 400 HV1, due to the inhomogeneity of microstructures. The impact absorbed energy of bonding interface sites in welds was considerably lower than that of base metal (about 20% of parent metal) because of the local obviously coarse grain, Widmanstätten ferrites, and banding ferrite defects. The principle of “close mode” friction welding is illustrated, and the microstructural characteristics and mechanical properties of welds can be predicted by judging the type of friction welding.

**Keywords** Friction taper plug welding · API X52 pipeline steel · Welding parameters · Microstructure · Mechanical properties

## 1 Introduction

Friction hydro-pillar processing (FHPP) is a solid-state welding process invented and patented by The Welding Institute (TWI) in 1992 [1]. It is also known as friction taper plug welding (FTPW) when conical hole and taper plug are used to perform the experiments. Before the welding process, a blind hole is drilled on the base plate. A plug with high rotational speed is inserted into the hole. The plug contacts with the hole under axial force generating heat because of mutual friction. A series of plasticized shear layers are

produced and fill the hole constantly. The welding process is finished when the consumption of plug comes to the set value and the plug stop rotation. Metallurgical bonding takes place between the plug and base plate under thermal-mechanical coupling. There are four important welding parameters during the welding process: rotational speed, axial force, forging force, and burn-off. Rotational speed is the spindle rotational speed which determines the relative movement of plug and hole. Axial force is the force applied on the plug during the welding process. Forging force is the force applied when the plug stops rotation. The burn-off is the consumption of plug during the welding process.

Unlike underwater arc welding, FHPP/FTPW which has the advantages of solid-state welding and is insensitive to water depth is considered as one of the most promising underwater join and repair technologies [2–6]. Some investigations of microstructure and mechanical properties on FHPP/FTPW have been reported. Unfried et al. [7] studied the microstructural evolution of friction taper plug-welded joints of C-Mn steels. Hattings et al. [8] investigated the process and metallurgy in phase transformation and fracture toughness of

---

Recommended for publication by Commission III - Resistance Welding, Solid State Welding, and Allied Joining Process

✉ Xinqi Yang  
xqyang@tju.edu.cn

<sup>1</sup> Tianjin Key Laboratory of Advanced Joining Technology, School of Materials Science and Engineering, Tianjin University, Tianjin 300072, People's Republic of China

**Table 2** Welding parameters

Sample number	Rotational speed (rpm)	Axial force (kN)	Forging force (kN)	Forging time (s)	Burn-off (mm)
A1	6500	30	35	5	14
A2	6500	35	40	5	14
A3	6500	40	45	5	14
A4	6500	45	50	5	14
B1	7000	30	35	5	14
B2	7000	35	40	5	14
B3	7000	40	45	5	14
B4	7000	45	50	5	14
C1	7500	30	35	5	14
C2	7500	35	40	5	14
C3	7500	40	45	5	14
C4	7500	45	50	5	14

**Table 1** Chemical composition of API X52 pipeline steel (wt%)

Grade	C	Si	Mn	P	S	Cu	Cr	Mo	V	Nb	Ti	Fe
X52	0.16	0.22	1.09	0.003	0.0068	0.028	0.042	0.096	<0.1	0.04	0.03	Bal.

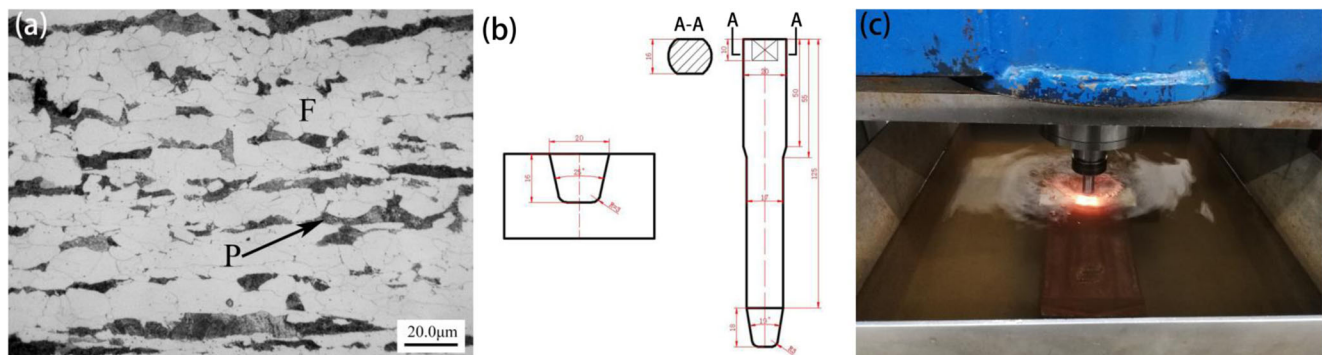
friction hydro-pillar processing welding in C-Mn steel. Meinhardt et al. [9] evaluated the microstructural, corrosion, and toughness properties of friction hydro-pillar processing-welded duplex stainless steels. Teng et al. [10] investigated the influence of heat treatment on microstructure and mechanical properties of underwater friction stitch-welded joints for DH36. Based on our previous work, defect-free joints were obtained with appropriate shapes of hole and plug and suitable welding parameters both in air and underwater and the mechanical properties of joints were evaluated [11, 12]. However, most of reports are concerned about FHPP/FTPW in air and the effects of welding parameters on microstructure and mechanical properties of wet FHPP/FTPW joints are rarely involved.

In the present study, the welded joint is divided into several regions taking the features of joint formation into account. The microstructures and mechanical properties (hardness and impact toughness) of the welded joints with different welding

parameters are observed and measured, respectively. Microstructural characteristics are carefully analyzed. Effects of the most important welding parameters, namely, rotational speed and axial force, on microstructure and mechanical properties are investigated. According to the particular microstructural characteristics and mechanical properties of welds, the terms of “Open Mode” Friction Welding, “Semi-open Mode” Friction Welding, and “Close Mode” Friction Welding are proposed to predict the microstructure and mechanical properties of FTP welded joints for low-alloy pipeline steel by judging the type of friction welding.

## 2 Materials and experimental procedures

Both of base material (BM) and plug used here was X52 pipeline steel. The microstructure of BM is characterized by

**Fig. 1** a Microstructure of BM. b Geometries of plug and hole. c Welding machine

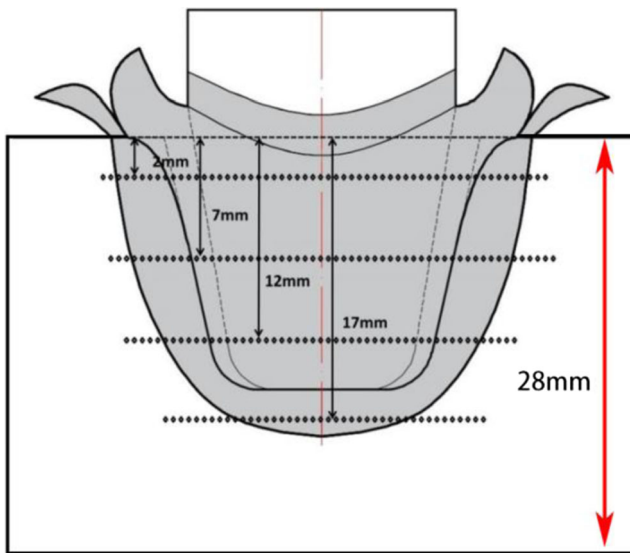


Fig. 2 Positions of hardness test points

polygonal ferrite with banded perlite, as shown in Fig. 1a. X52 pipeline steel is a kind of high-strength low-alloy (HSLA) steel with high strength and excellent toughness. The chemical composition and mechanical properties of X52 pipeline steel are shown in Table 1.

According to our previous research work [13], a group of plug and hole with fixed shape and size was selected to perform FTPW experiments. The specific geometries of plug and hole are shown in Fig. 1b. The FTPW experiments were carried on a machine designed and developed by Tianjin University in 2012. The plug and base plate were completely immersed in water to simulate a wet welding condition, as shown in Fig. 1c. There are four important welding parameters: rotational speed, axial force, forging force, and burn-off. Welded joints with different welding parameters were

obtained with rotational speed ranging from 6500 to 7500 rpm and axial force varying from 30 to 45 kN. The forging force was set 5 kN larger than axial force. And the forging time and burn-off were set as fixed values of 5 s and 14 mm, respectively, as shown in Table 2.

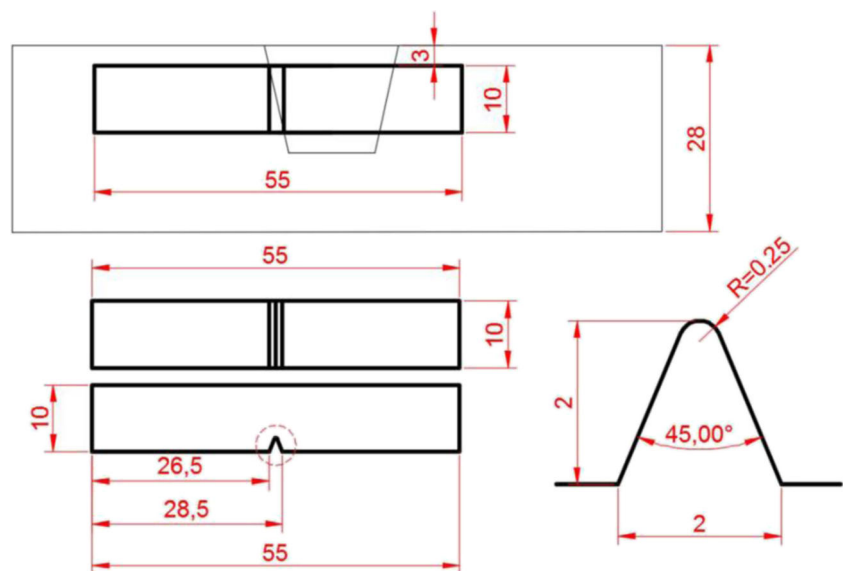
The metallographic samples were cut from welded joints, grinded with #240–#2000 abrasive paper, mechanically polished, and etched with 3% nitric alcohol finally. The welding defects and microstructure of welded joints were observed by OLYMPUS-GX51F optical microscope and TDCL-S4800 scanning electron microscope. The hardness tests were performed on metallographic samples with 0.5-mm interval distance between each test point at 2, 7, 12, and 17 mm below the top surface of base plate, as shown in Fig. 2. The Charpy impact experiments of FTP welds with V-notch in the bonding zone were operated at 0 °C based on the impact test standard. The detailed geometry of impact specimen is shown in Fig. 3.

### 3 Results and discussions

#### 3.1 Division and microstructural characteristics

It can be observed from Fig. 4 that plug and hole have approximately kept their original shapes after welding process. The bonding zone (BZ) between plug and hole is distinct. Microstructure of joint is totally different from BM because of the complicated thermal-mechanical coupling effects. According to the characteristics of joint formation, the joint can be divided into forged zone (FZ), final frictional plane (FFP), bonding zone (BZ), and heat-affected zone (HAZ). The HAZ includes two parts: base material HAZ (BM HAZ) and taper plug HAZ (TP HAZ). The HAZ is located between

Fig. 3 Geometry of impact specimen with V-notch in bonding zone



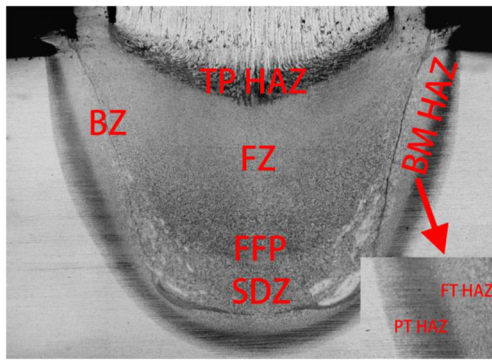


Fig. 4 Division of joint

BM and BZ with temperature ranging from room temperature to elevated temperature, so that the change of microstructure in HAZ is significant. Based on the distinctions of microstructure, BM HAZ or TP HAZ can be subdivided into two sub-regions: partially transformed HAZ (PT HAZ) and fully transformed HAZ (FT HAZ). PT HAZ contains untransformed polygonal ferrite (UPF). The microstructural characteristics of the two regions will be discussed in detail below.

Shear deformation zone (SDZ) is made of a series of plasticized shear layers which is generated due to severe frictional shear deformation under axial force. There is a distinct extruding flow tendency from the center to two sides in SDZ. The frictional interface rises with the welding time. Final frictional interface (FFP) is located in the plane where the friction interface stays when the FTPW process is completed. FFP divides the weld region into two parts: the upper region and the lower region. The two regions refer to FZ and SDZ, respectively, and the microstructure of FZ is more uniform as compared to SDZ. Bonding zone refers to the bonding interface and represented as a line due to its narrow width.

Some special white blocks are also observed around frictional interface. They are proved to consist of a large fraction

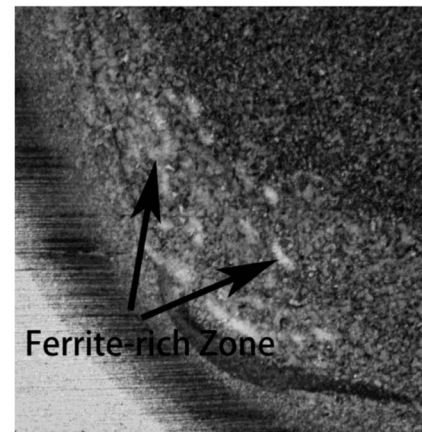
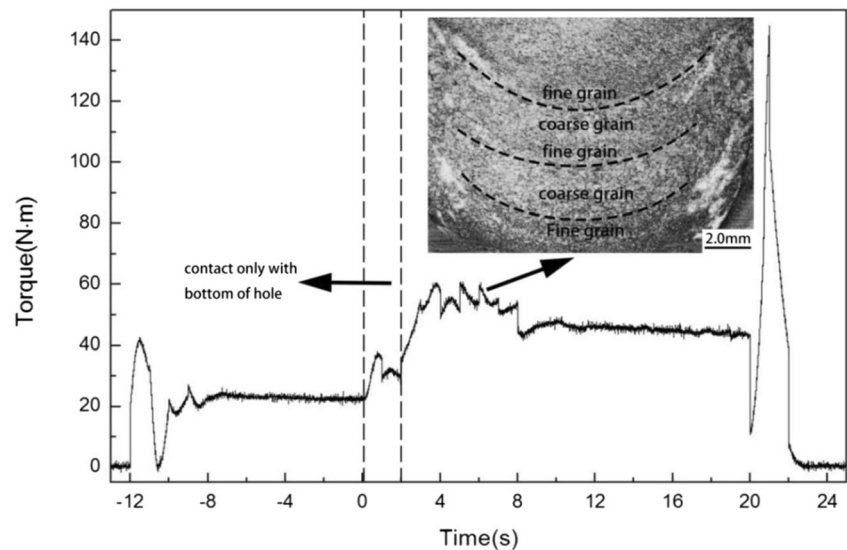


Fig. 5 Ferrite-rich blocks in SDZ

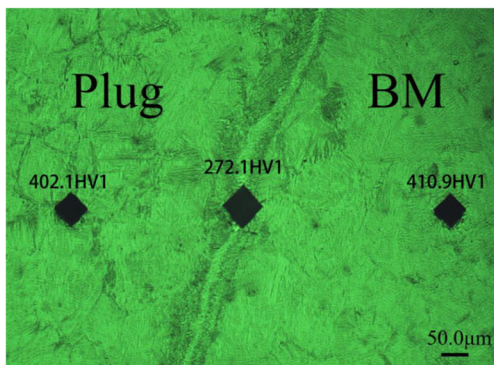
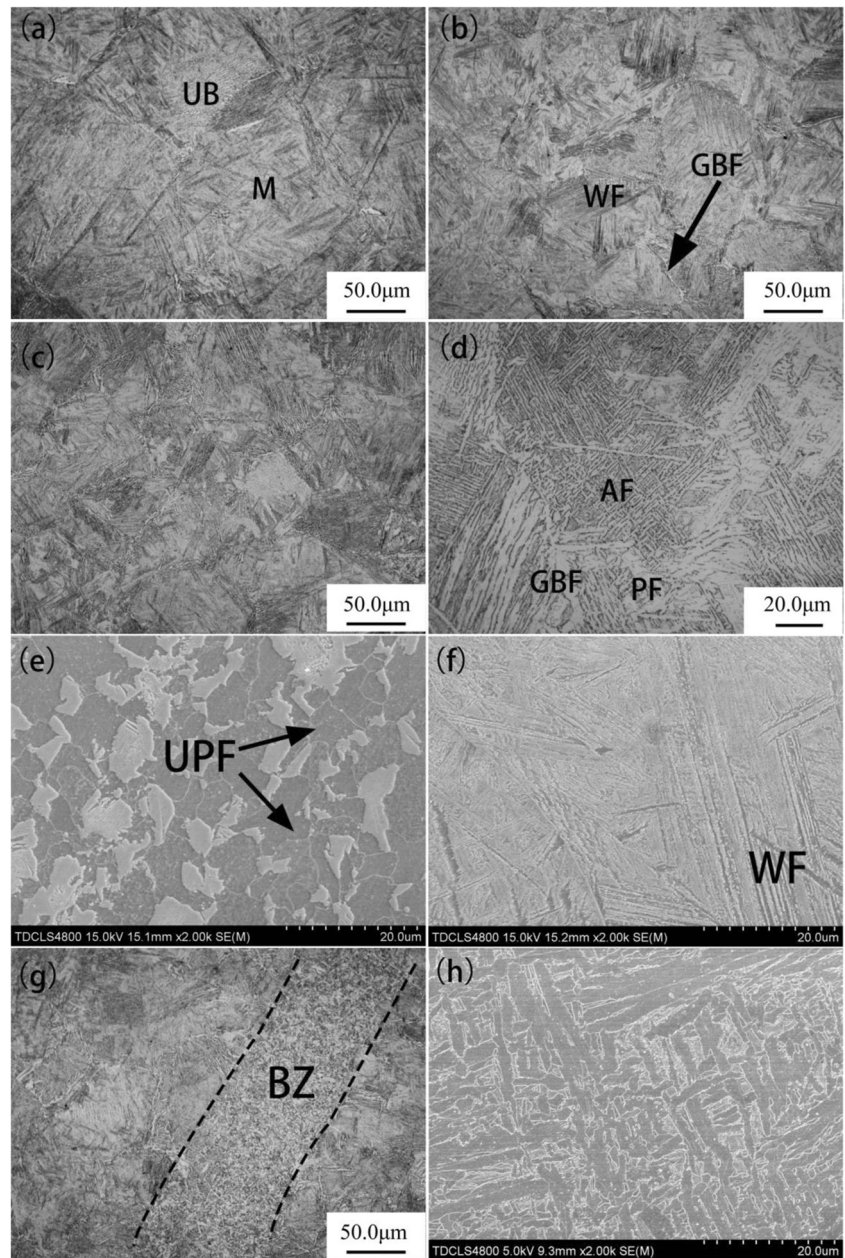
of ferrite and are called ferrite-rich blocks, as shown in Fig. 5. The formation of ferrite-rich blocks should be related to decarburization which is caused by the reaction between the local steam with high temperature and high-temperature plasticized steel, as shown below. The ferrite-rich blocks distributes non-uniformly in SDZ because the temperature in SDZ is inhomogeneous and the shape and size of frictional interface change constantly.

Figure 6 shows the measured torque during the welding process. At the initial stage of process, the torque is low because the plug contacts only with bottom of the hole. Subsequently, the plug starts to contact with the sidewall of the hole, so that torque increases drastically owing to a larger contact area. In addition, the torque fluctuates as frictional interface moves to create the set axial force on the new frictional plane which has higher strength with lower temperature due to being far away from previous frictional planes. Thus, the frictional planes can be identified by the torque fluctuation. Also, the layered structure with alternative fine grain and

Fig. 6 The measured torque during the welding process



**Fig. 7** Microstructure of **a** FZ, **b** FFP, **c** SDZ except for ferrite-rich block, **d** ferrite-rich block, **e** PT HAZ, **f** FT HAZ, **g** BZ, and **h** magnification of BZ



**Fig. 8** Hardness comparison of BZ and its vicinity

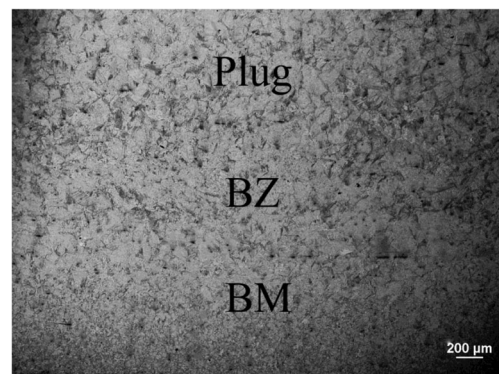


**Fig. 9** BZ at the bottom center

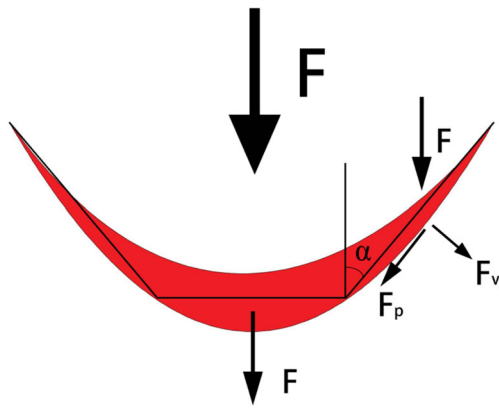


**Fig. 10** Stress state during the welding process

coarse grain in SDZ due to inhomogeneous shear deformation and temperature is consistent with the torque fluctuation.

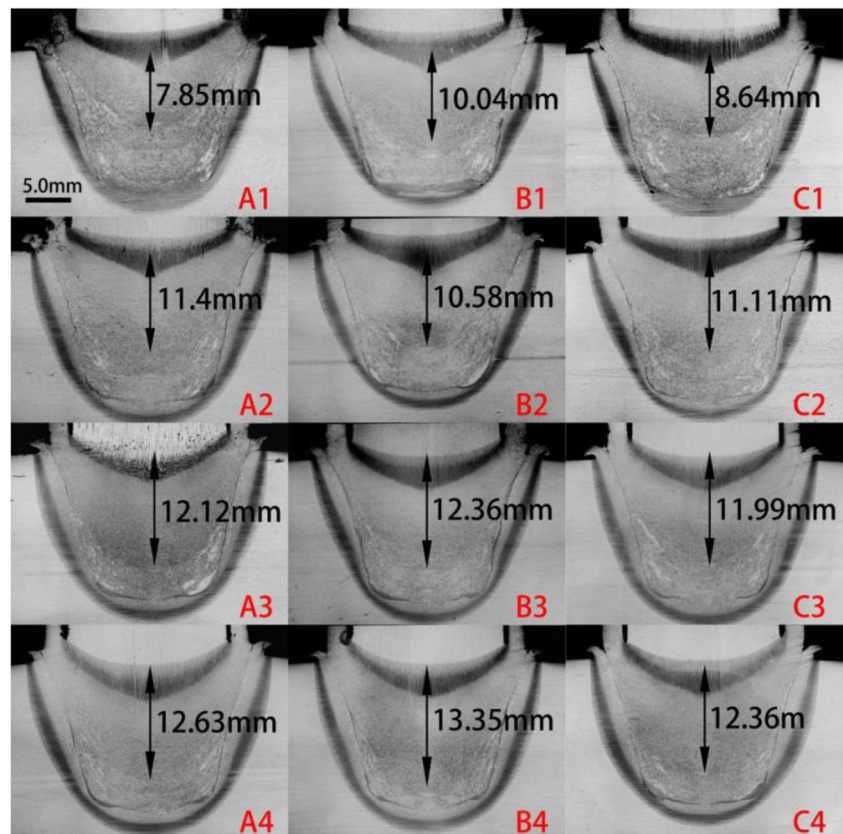
FZ mainly consists of martensite (M) and small amounts of upper bainite (UB) and nearly no grain-boundary ferrite (GBF), as shown in Fig. 7a. FFP is dominantly characterized by martensite (M), upper bainite, slender grain-boundary ferrite (GBF), and widmanstätten ferrite (WF). Ferrite-rich blocks are made of various types of ferrites, including grain-boundary ferrite (GBF), polygonal ferrite (PF), and Widmanstätten ferrite (WF). Except for ferrite-rich blocks, the rest of SDZ has the similar microstructure to FFP.

Figure 7e, f shows the SEM graph of microstructure in HAZ. The PT HAZ contains untransformed polygonal ferrite (UPF) with the peak temperature below  $A_{c3}$ . FT HAZ mainly consists of coarse martensite and small amounts of Widmanstätten ferrite (WF) in the grain boundary. This is because that austenite grains become astonishingly coarse with the peak temperature much higher than  $A_{c3}$  and transform into coarse martensite and Widmanstätten ferrite (WF) due to water cooling. BZ is a band with fine-grained ferrite, as shown in Fig. 7g, h. As mentioned above, this result may be caused by local decarbonization and recrystallization [14]. In addition, the diffusion of  $H_2$  produced by decarburization may result in hydrogen embrittlement which has a huge impact on the toughness of welds.

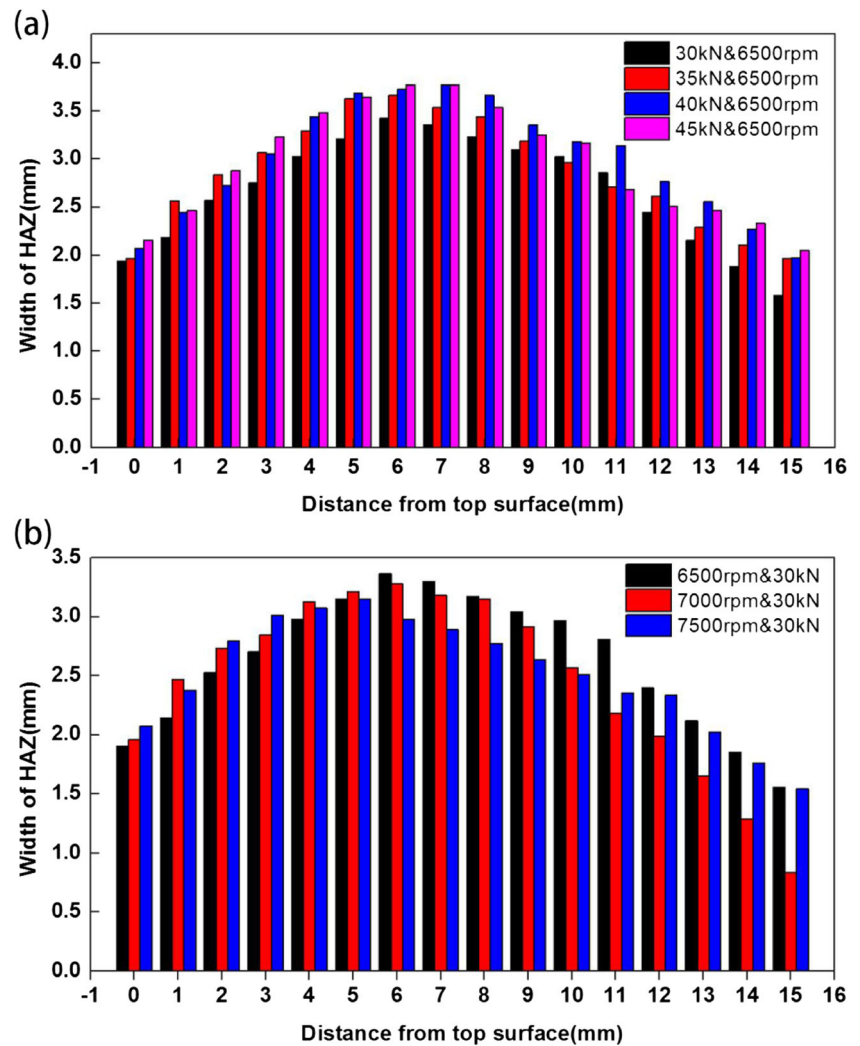
Figure 8 shows the hardness comparison of BZ and its vicinity. The hardness of BZ (272.1 HV1) is much lower than its vicinity (more than 400 HV1), which is consistent with microstructure. Because of the narrow width and low hardness and strength, BZ is the weak area for the whole welded joint and should play a role similar to fissure defect and has important influences on the toughness of joint.

Figure 9 shows the bonding zone (BZ) at the bottom center. The BZ at the bottom center cannot be observed clearly which is very different from the BZ to the side. The behavior is closely related to the difference of stress state. During the welding process, the frictional interfaces change to

**Fig. 11** Distance from FFP to top surface



**Fig. 12** Effect of **a** axial force and **b** rotational speed on width of HAZ



hemispherical shape. The axial force applied on the sidewall can be divided into two parts: the parallel part  $F_p$  and the vertical part  $F_v$ , and the vertical part  $F_v$  is the actual force applied on the sidewall.

$$F_v = F \cdot \sin\alpha$$

Because  $\alpha$  is a small angle, the force on the sidewall  $F_v$  is much lower than that at the bottom center, as shown in Fig. 10. Thus, the formation mechanism of BZ at the bottom center differs from that of BZ to the side.

### 3.2 Effects of welding parameters on microstructure

The geometries of welds with different welding parameters are similar. Figure 11 shows the distances from FFP to top surface of the welded joints. The distance from FFP to top surface increases drastically with higher axial force from less

8 mm to more than 12 mm. Rotational speed does not seem to have significant influence on distance from FFP to top surface.

From top surface to the bottom of joint, BM HAZ width increases from approximately 2 mm to more than 3 mm, decreases subsequently, and minimizes at the rounded transition. These behaviors are related to welding process and cooling condition. The top surface is contacted with water directly with a rapid cooling rate resulting in a narrow HAZ width at the top surface. The minimum HAZ width at the rounded transition is caused by the rapid cooling at the initial stage of welding process. Figure 12a, b shows the effects of axial force and rotational speed on HAZ width, respectively. Both of axial force and rotational speed have no significant influence on HAZ width. However, higher axial force contributes to shorter distance from FFP to the bottom. Thus, the HAZ width reduces much slower.

Figure 13a illustrates the significant effects of axial force on area ratio of SDZ and FZ. With axial force increasing from 30 to 45 kN, area ratio of SDZ decreases from above 40 to

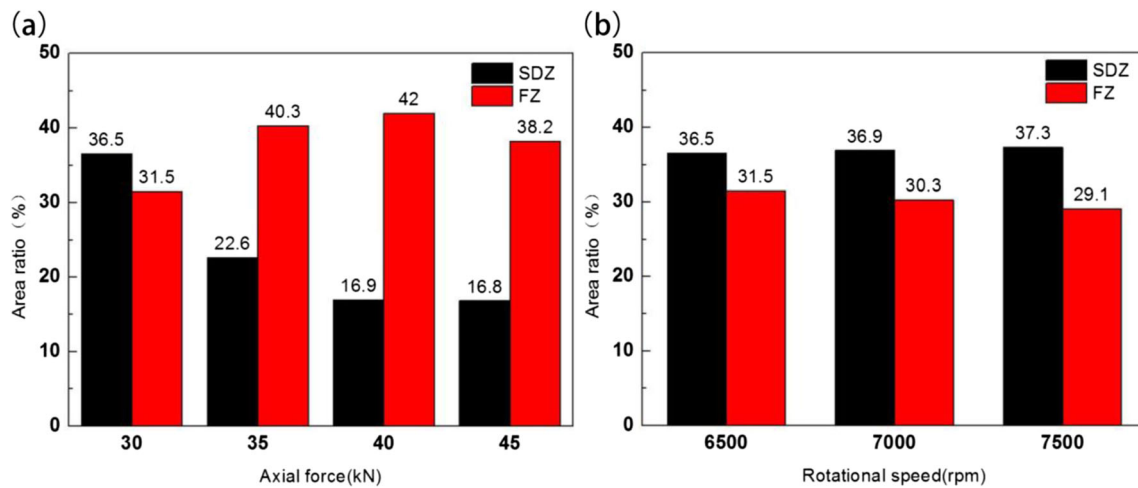


**Fig. 13** Area ratio of different regions in welded joints of **a** A1–A4 and **b** A1, B1, and C1

below 17% as the final frictional plane is closer to the bottom. The area ratio of FZ increases firstly, and then decreases with higher axial force. This is because the TP HAZ is also closer to bottom with higher axial force. With the same axial force, however, the area ratio of SDZ and FZ varies little at different rotational speeds, as shown in Fig. 13b.

Figure 14 shows the microstructure of ferrite-rich blocks with 7000-rpm rotational speed at various axial forces. For lower axial force, PF and GBF prefer to be generated in SDZ, while BGF and AF tend to be produced in SDZ with high axial force. With axial force increasing, both the fraction and size of ferrite decrease. These behaviors can be explained considering that lower axial force contributes to longer welding time for ferrite to grow up to coarse PF or ferrite lath and fine needle-like ferrite is depressed to grow up for short welding time when using high axial force to perform FTPW

experiment. Thus, it can be inferred that the increasing axial force should be beneficial to decrease the amount of ferrite-rich blocks, and thus to reduce the effects of decarbonization. In summary, axial force has a greater effect on microstructure of welded joints as compared to rotational speed.

### 3.3 Effects of welding parameters on mechanical properties

#### 3.3.1 Hardness

Figure 15 shows the hardness profile (HV1) measured on the cross section of welded joints with 7500-rpm rotational speed at 35-kN axial force. It is shown that hardness of BM is about 200 HV1 and the hardness sharply increases to more than 400 HV1 in the HAZ. BZ mainly consisting of fine grain

**Fig. 14** Microstructure of ferrite-rich block at different axial forces. **a** 30 kN. **b** 35 kN. **c** 40 kN. **d** 45 kN

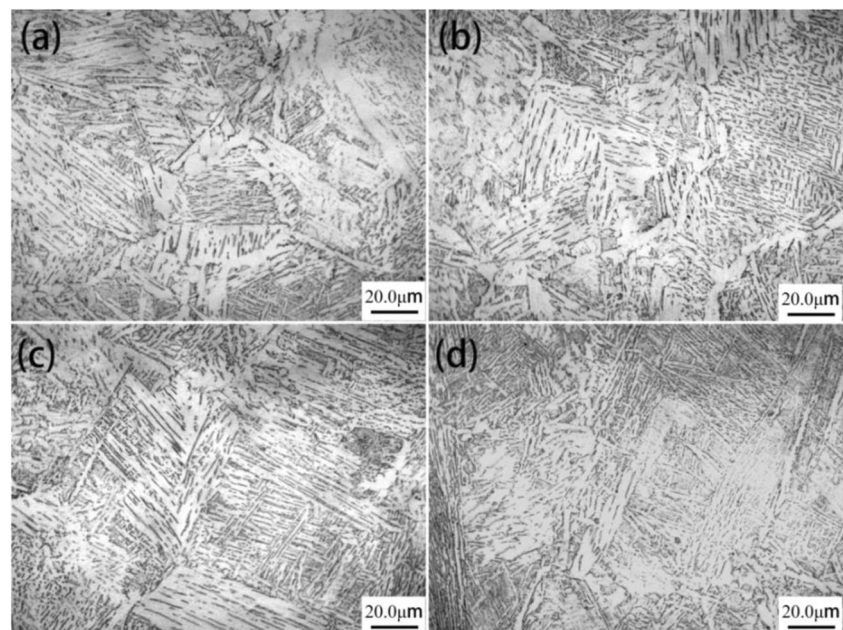
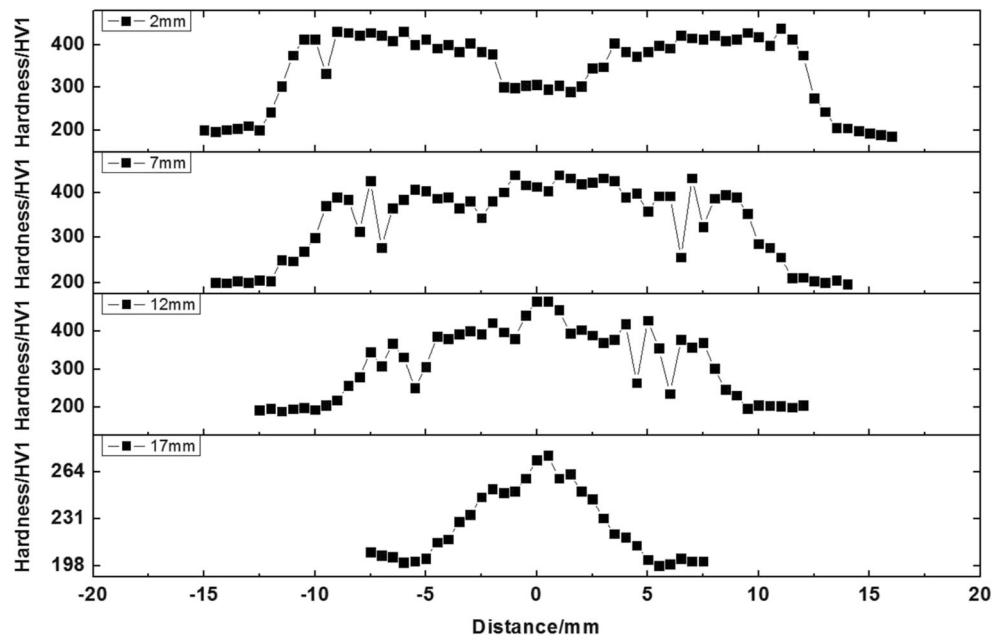




**Fig. 15** Hardness profiles of welded joints with 7500-rpm rotational speed at 35-kN axial force



ferrite as mentioned above is a narrow soft region, leading to a decrease in hardness. In PT HAZ, due to the refinement of grain and the increasing fraction of martensite, the hardness considerably grows. Unlike PT HAZ, the increase of hardness in FT HAZ is caused by martensite generation completely. Hardness of the center at 2 mm below top surface of welded joint is low because of relatively flat thermal cycle. The behavior that the hardness in SDZ (7 and 12 mm below top surface) fluctuates dramatically is closely related to the mixing microstructures in SDZ. Ferrite-rich blocks dominantly consisting of polygonal ferrite and acicular ferrite have a low hardness, but hardness of the rest in SDZ is considerably higher due to the existence of martensite. The significant increase in hardness of the center at 12 mm below top surface of welded joints may be due to the fact that the region lies right in FFP with finer grains. The hardness at 17 mm below top surface is relatively lower because of the long distance from friction interface (heat source) resulting in much smaller heat input at the beginning of welding process.

Figure 16a depicts hardness distribution at 2 and 7 mm below top surface with 30–45-kN axial forces at the same rotational speed of 7000 rpm. It is clearly observed that the hardness in the center of plug weld at 2 mm below top surface is lower with increasing axial force. This behavior is caused by the fact that the final frictional interface is closer to the bottom of hole with higher axial force. Lower axial force leads to a longer welding time and a larger heat input during the welding process, resulting in a more intensive fluctuation of hardness profile in SDZ. Figure 16b shows hardness distribution of welded joints with 6500–7500-rpm rotational speed at the same axial force of 35 kN. The hardness changes little with the variation of rotational speed, concluding that rotational

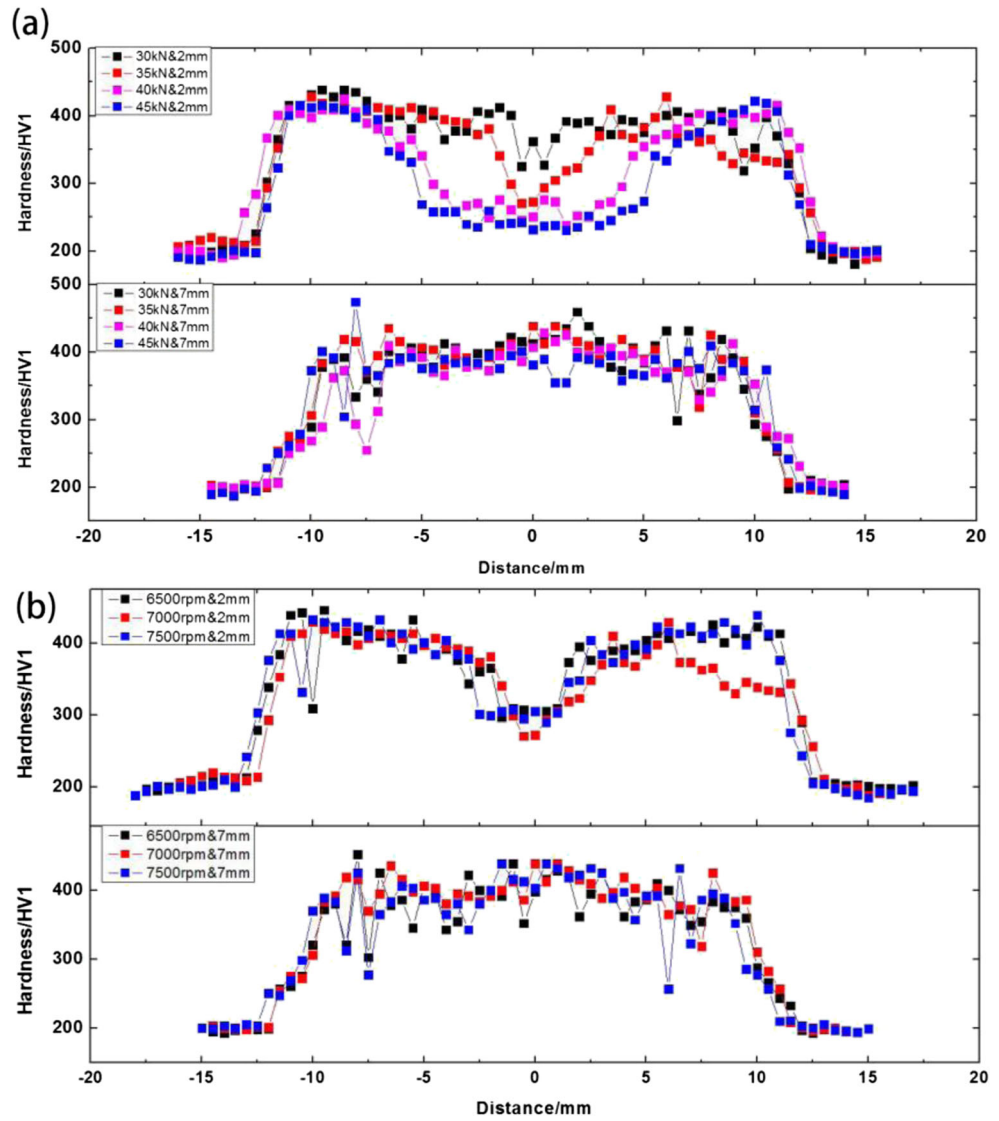
speed has little influence on hardness of welded joints. In summary, the microhardness of weld region is obviously higher than that of base material.

### 3.3.2 Impact toughness

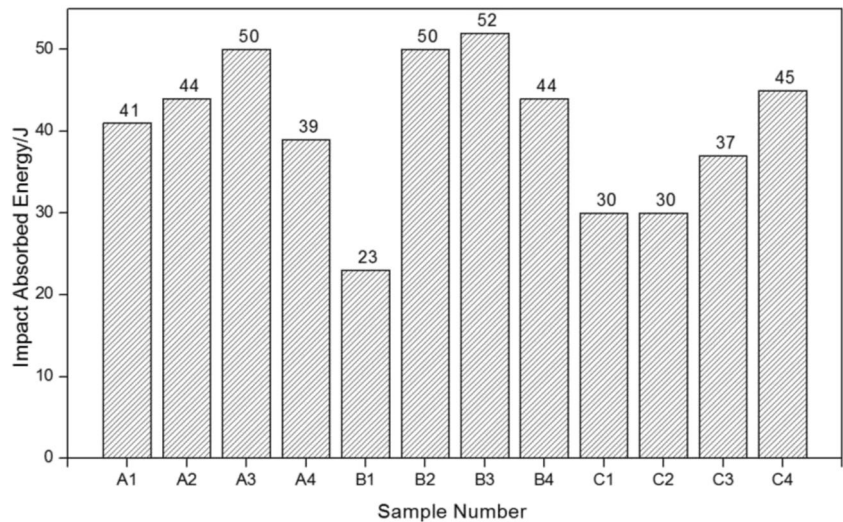
The impact absorbed energy of welds in BZ with different welding parameters was measured, as shown in Fig. 17. The impact absorbed energy of welded joints which varies from 23 to 52 J, only about 20% of parent metal (267 J), displaying a huge difference from that of BM. At the same rotational speed of 6500 or 7000 rpm, the impact-absorbed energy of welded joint increases first with axial force increasing, and then decreases. However, the impact-absorbed energy of welded joint always rises with the axial force when the rotational speed is high (7500 rpm). It is found that the welded joint generally displays better performance when high rotational speed matches with large axial force and low rotational speed matches with low axial force.

Figure 18 shows the fracture morphologies of base material and welded joint. Base material fractured in the middle of V-notch. However (Fig. 18a), for the welded joints obtained with different rotational speeds and axial forces, crack initiates at the BZ and/or the HAZ and propagates along the bonding zone during the Charpy impact test, as shown in Fig. 18b. These behaviors have close relationship with microstructural features. The fracture morphology of base material consists of huge dimples and obvious deformation can be observed, as shown in Fig. 18c. These characteristics are consistent with high-impact absorbed energy of base material. Unlike base material, the fracture morphology of welded joint contains

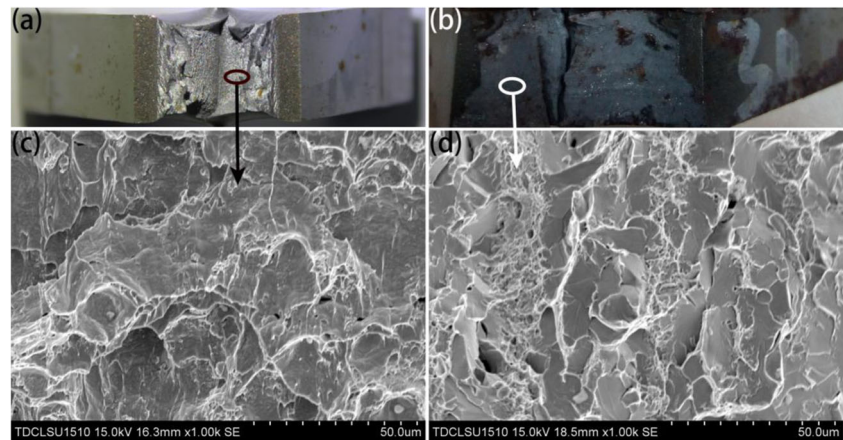
**Fig. 16** **a** Hardness distribution of welded joints with 30–45-kN axial force at the same rotational speed of 7000 rpm and **b** with 6500–7500-rpm rotational speed at the same axial force of 35 kN



**Fig. 17** Impact absorbed energy of welded joints with different welding parameters



**Fig. 18** Fracture morphology of a, c BM and b, d welded joint



not only small dimples but also river-like patterns, belonging to a compound fracture mode, as shown in Fig. 18d.

### 3.4 The principle of “close mode” friction welding

According to the above analysis and discussions, it is found that the microstructure of underwater wet FTP-welded joint is significantly inhomogeneous and contains dramatically coarse grains showing a big difference with traditional friction welding such as continuous drive friction welding which is characterized by fine-grained microstructure. These behaviors are closely related to the forming process and bonding mechanism of welded joint. During the continuous drive friction welding process, the overheated metal is extruded out to form flash which is removed subsequently by machining technology. However, during the FHPP/FTPW welding process, the overheated metal was sheared and extruded to fill the gap between the hole and plug during the FHPP/FTPW joining the plug and hole and becomes a part of the joint due to the constraint and containment of hole.

Therefore, we propose the terms of “Open Mode” Friction Welding (OMFW), “Semi-open Mode” Friction Welding (SOMFW), and “Close Mode” Friction Welding (CMFW), as shown in Fig. 19. Most of traditional friction welding processes belong to OMFW. The flashes are generated at both of upside and downside because the frictional interface is completely open and unconstrained. The flashes are removed so that the joint with fine grains shows excellent performance.

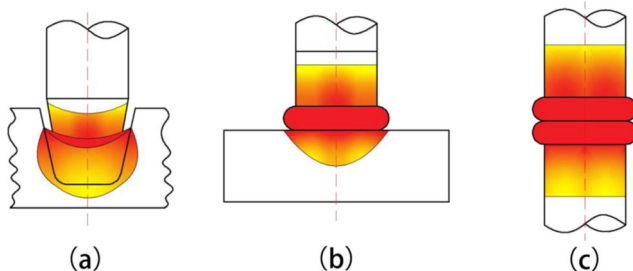


**Fig. 19** a CMFW. b SOMFW. c OMFW

Friction surfacing belongs to SOMFW and the flash is formed at only one side and then removed, which would inevitably affect the microstructure of surfacing layer. FHPP/FTPW belongs to CMFW during which the flash with elevated temperature turns into a part of joint. Thus, the microstructure of joint shows extreme inhomogeneity and the mechanical properties, especially toughness, of joints significantly decrease. The reduction of plasticity and toughness for friction taper plug-welded joints will be a role to restrict the wide application of FTPW in marine engineering steel. With the terms of OMFW, SOMFW, and CMFW, the microstructural characteristics and mechanical properties of welds can be predicted by judging the type of friction welding for low-alloy pipeline steel.

## 4 Conclusion

Microstructure and mechanical properties of underwater wet FTP-welded joints with different welding parameters are observed and measured, respectively. The main conclusions are summarized as follows:

- (1) The weld region could be divided into forged zone (FZ), final frictional plane (FFP), shear deformation zone (SDZ), bonding zone (BZ), and heat-affected zone (HAZ). The layered structure of plug weld can be identified by the torque fluctuation. The microstructure of joint is remarkably inhomogeneous and very different from base material. The HAZ has coarse grains and mainly consists of martensite and Widmanstätten ferrite. Ferrite-rich blocks in SDZ are made of various types of ferrites, including grain-boundary ferrite (GBF), polygonal ferrite (PF), and Widmanstätten ferrite (WF). BZ is a band with fine-grained ferrite and a weak area for whole welded joint, playing a role similar to fissure defect owing to the narrow width and low hardness and strength.
- (2) Compared with rotational speed, axial force has a greater impact on microstructure of welded joint. The hardness

profiles measured on cross section of welded joints are severely non-uniform, ranging from 200 to 400 HV1, due to the inhomogeneity of microstructures. The impact-absorbed energy of bonding interface sites in welds was considerably lower than that of base metal (about 20% of parent metal) because of the local obviously coarse grain, Widmanstätten ferrites, and banding ferrite defects.

- (3) According to the formation characteristics of various welding techniques, we propose the terms of OMF, SOMF, and CMF. With the terms of OMF, SOMF, and CMF, the microstructural characteristics and mechanical properties of welds can be predicted by judging the type of friction welding.

**Funding** The authors acknowledge the financial support from National Natural Science Foundation of China (51475327).

## References

1. Thomas WM, Ichniowski ED, Jones SR et al (1993) Friction forming: International Patent, WO 93/04813[P]
2. Nixon J (2000) Underwater repair technology. Abington Publishing, Cambridge
3. Łabanowski J, Fydrych D, Rogalski G (2008) Underwater welding - a review. *Adv Mater Sci* 8(3):11–22
4. Meyer A (2003) Friction hydro pillar processing: bonding mechanism and properties. GKSS- Forschungszentrum Geesthacht GmbH, Hamburg
5. Han B, Huang Y, Lv S, Wan L, Feng J, Fu G (2013) AA7075 bit for repairing AA2219 keyhole by filling friction stir welding. *Mater Des* 51(5):25–33
6. Han R, Ji S, Meng X et al (2018) Drilling-filling friction stir repairing of AZ31B magnesium alloy. *J Mater Process Technol* 255:765–772
7. Unfried JS et al (2010) Study of microstructural evolution of friction taper plug welded joints of C-Mn steels. *Sci Technol Weld Join* 15(6):506–513
8. Hattingh DG, Bulbring DLH, Els-Botes A, James MN (2011) Process parameter influence on performance of friction taper stud welds in AISI 4140 steel. *Mater Des* 32(6):3421–3430
9. Meinhardt CP, Chludzinski M, Ribeiro RF, Rocha CLF, Santos ACS, Strohaecker TR (2017) Evaluation of friction hydro-pillar processing welding in duplex stainless steels (UNS S31803). *J Mater Process Technol* 246:158–166. <https://doi.org/10.1016/j.jmatprotec.2017.03.010>
10. Teng J, Wang D, Wang Z, Zhang X, Li Y, Cao J, Xu W, Yang F (2017) Repair of arc welded DH36 joint by underwater friction stitch welding. *Mater Des* 118:266–278
11. Yin Y et al (2014) Welding process and microstructure of weld for friction hydro pillar welded DH36 high strength steel. *Trans China Weld Inst* 35(9):109–114
12. Cui L, Yang X, Wang D, Cao J, Xu W (2014) Experimental study of friction taper plug welding for low alloy structure steel: welding process, defects, microstructures and mechanical properties. *Mater Des* (1980–2015) 62:271–281
13. Hou X (2013) Research on the experiments and the microstructure properties of friction hydro pillar processing. Tianjin University, Tianjin
14. Yin Y, Yang X, Cui L, Wang F, Li S (2015) Material flow influence on the weld formation and mechanical performance in underwater friction taper plug welds for pipeline steel. *Mater Des* 88:990–998